Journal of the Neurological Sciences 443 (2022) 120458

Contents lists available at ScienceDirect

Journal of the Neurological Sciences

journal homepage: www.elsevier.com/locate/jns

The human brain networks mediating the vestibular sensation of self-motion

Zaeem Hadi [a,*], Mohammad Mahmud [a], Yuscah Pondeca [a], Elena Calzolari [a], Mariya Chepisheva [a], Rebecca M. Smith [a], Heiko M. Rust [a,c], David J. Sharp [b], Barry M. Seemungal [a,*]

[a] Centre for Vestibular Neurology, Department of Brain Sciences, Imperial College London, UK
[b] Computational, Cognitive and Clinical Neuroimaging Laboratory, Department of Brain Sciences, Imperial College London, UK
[c] Neurology, Universitätsspital Basel, Basel, Switzerland

ARTICLE INFO

Keywords:
Self-motion perception
Vestibular agnosia
Vestibular cognition
Vertigo
Resting-state functional connectivity
Traumatic brain injury

ABSTRACT

Vestibular Agnosia - where peripheral vestibular activation triggers the usual reflex nystagmus response but with attenuated or no self-motion perception - is found in brain disease with disrupted cortical network functioning, e.g. traumatic brain injury (TBI) or neurodegeneration (Parkinson's Disease). Patients with acute focal hemispheric lesions (e.g. stroke) do not manifest vestibular agnosia. Thus, brain network mapping techniques, e.g. resting state functional MRI (rsfMRI), are needed to interrogate functional brain networks mediating vestibular agnosia. Hence, we prospectively recruited 39 acute TBI patients with preserved peripheral vestibular function and obtained self-motion perceptual thresholds during passive yaw rotations in the dark and additionally acquired whole-brain rsfMRI in the acute phase. Following quality-control checks, 26 patient scans were analyzed. Using self-motion perceptual thresholds from a matched healthy control group, 11 acute TBI patients were classified as having vestibular agnosia versus 15 with normal self-motion perception thresholds. Using independent component analysis on the rsfMRI data, we found altered functional connectivity in bilateral lingual gyrus and temporo-occipital fusiform cortex in the vestibular agnosia patients. Moreover, regions of interest analyses showed both inter-hemispheric and intra-hemispheric network disruption in vestibular agnosia. In conclusion, our results show that vestibular agnosia is mediated by bilateral anterior and posterior network dysfunction and reveal the distributed brain mechanisms mediating vestibular self-motion perception.

1. Introduction

We recently characterized a clinical syndrome called vestibular agnosia (VA) in patients with acute traumatic brain injury (TBI), where, despite preserved peripheral and reflex vestibular functioning, patients had an attenuated vestibular-mediated sensation of self-motion ('vestibular-motion perception') [5]. Vestibular agnosia has also been recorded in elderly patients, typically with small vessel disease and imbalance [7,29,52], and in patients with advanced Parkinson's Disease with falls [65]. We recently showed that in acute TBI patients with imbalance, objective measures of VA correlate with impaired white matter structural integrity in the right inferior longitudinal fasciculus (ILF) [5]. This structural analysis thus identified the overlap in imbalance and VA, however the neural correlates distinct to VA were not identified.

There is evidence to support the notion that self-motion perception is not localizable [68]. We previously showed that the duration of motion-perception sensation in the dark (elicited by a rapid stop from constant angular rotation) in healthy individuals correlated with a widespread, bilateral white matter network [42]. Subsequent tractography studies also showed that vestibular networks are bihemispherically linked via the corpus callosum [32,61]. In support of a distributed coding for self-motion perception is the lack of effect of acute focal lesions (stroke - [31]) or via non-invasive stimulation [54] on vestibular-motion perception.

Previous work suggests that an anterior and a posterior thalamocortical pathway convey vestibular signals to cortical circuits mediating vestibular functions including self-motion perception and spatial

* Corresponding authors at: Centre for Vestibular Neurology, Department of Brain Sciences, Imperial College London, UK.
E-mail addresses: zhadi@ic.ac.uk (Z. Hadi), bmseem@ic.ac.uk (B.M. Seemungal).

https://doi.org/10.1016/j.jns.2022.120458
Received 3 May 2022; Received in revised form 18 September 2022; Accepted 11 October 2022
Available online 15 October 2022

orientation [8]. The anterior pathway originates from vestibular nuclei and projects to regions including the hippocampus via anterior-dorsal thalamus and entorhinal cortex [8,26]. The hippocampus projects to pre-frontal brain regions [55,62], and these long-range (hippocampal-prefrontal) projections have been reported to mediate the saliency of sensory stimuli for attentional networks [55]. The posterior thalamo-cortical pathway, primarily projects to posterior cortical brain region i.e., parieto-insular vestibular cortex (PIVC), which previously has been linked to the processing of self-motion [36].

Generally, posterior brain networks are considered to encode sensory inputs whereas anterior networks encode higher order functions and integrate sensory inputs [18]. This large-scale coordination of brain networks has been shown in spatial and visual sensory modalities in primates and humans, where sensory processing and integration is associated with unique activation within parietal regions (intra-network) and a distinct activation of fronto-parietal (inter-) networks [15,19,21]. Similar unique activations associated with anterior-integrative and posterior-sensory processing networks, and large scale anterior-posterior inter-network connectivity has been linked to cross-modal sensory perception disorders [16]. Accordingly, we postulated that there are (at least) two main cortical networks mediating VA; a posterior cortical network, receiving the main bottom-up vestibular signals mediating sensory processing, and an anterior cortical network linked to sensory integration, which in turn then triggers perception via 'perceptual ignition' mechanism [10]. Thus, dysfunction of the posterior network could result in loss of perception via impaired afferent signal processing; whereas a sensory integration dysfunction in anterior networks could also mediate VA.

Currently no study has shown the brain regions specifically associated with impaired self-motion perception with intact peripheral functioning (i.e. VA). Our general objective was to identify brain regions associated with VA. Moreover, to test our postulate of an anterior-posterior cortical network mediating VA, we hypothesize that VA in acute TBI is mediated by multi-network dysfunction, i.e. (i) by impaired functional connectivity within anterior networks, (ii) impaired functional connectivity within posterior networks, and (iii) inter-network impaired functional connectivity. In addition, we previously showed that VA is linked to imbalance via damage to the right inferior longitudinal fasciculus (ILF) [5]. Previous reports using diffusion imaging and tractography show that the ILF has its strongest structural link with the mid temporal and the lingual gyri and secondly with the calcarine gyrus [45]. The presence of these connections has also been confirmed in another study via white-matter dissection and tractography in humans [34]. Both, mid temporal and lingual gyri are reported to induce sensations of rotational motion in response to electrical stimulation [30], and additionally, the lingual gyrus (V3v/V4v) and calcarine region (V2) both display increased functional connectivity with galvanic vestibular stimulation [12]. We thus predict that damage to the ILF will result in altered functional connectivity in the mid temporal gyrus, lingual gyrus, and calcarine gyrus. To assess our hypotheses, we evaluated functional connectivity via resting state fMRI in both grey and white matter functional brain networks.

2. Material and methods

2.1. Patient recruitment

The data reported in this paper was collected as part of an MRC-funded prospective study [5]. 146 acute TBI patients were clinically assessed from whom 39 (Mean age ± SD: 41.64 ± 13) were recruited from the St Mary's Hospital Major Trauma Centre (London, UK) and King's College Hospital (London, UK). Inclusion Criteria were: (i) blunt head injury resulting in admission to the major trauma ward; (ii) age 18–65; (iii) preserved peripheral vestibular function. Exclusion criteria were: (i) additional active pre-morbid medical, neurological, or psychiatric condition (unless inactive or controlled); (ii) musculoskeletal condition impairing ability to balance; (iii) substance abuse history; (iv) pregnancy; and (v) inability to obtain consent or assent. Thirty-seven matched healthy controls were also recruited following written informed consent. The study was conducted in accordance with the principles of the Declaration of Helsinki and was approved by the local Research Ethics Committee.

2.2. Procedure

All participants completed assessment of peripheral and reflex vestibular function, vestibular perceptual testing, reaction times, posturography, neuroimaging, and questionnaires for perceived balance, and cognitive examination. The details for all tests have been reported previously [5]. Procedures involved in assessment of peripheral vestibular dysfunction, vestibular perceptual testing, posturography, and resting-state scans are listed here.

2.3. Assessment of peripheral vestibular function

Patients were assessed for their peripheral vestibular function to exclude peripheral dysfunction as a cause of impaired vestibular perception. Video head impulse testing and rotational chair testing with eye movement assessment of VOR gain for the stopping response from 90°/s constant rotation was used to assess peripheral dysfunction. All TBI patients included in the study had intact peripheral vestibular function [5].

2.4. Vestibular perceptual threshold

Vestibular perceptual thresholds were determined as a measure of self-motion perception and to classify subjects having abnormal perceptual thresholds with VA [5,52,53]. Fig. 1 shows the apparatus and method used to determine participants' vestibular-perceptual thresholds during passive yaw-plane rotations in the dark [53]. Participants sat on a rotating chair in the dark and were instructed to press either a right or left button as soon as they perceived a rotation in the respective direction (Fig. 1A and Fig. 1B). Lights were turned on after each trial in order to allow post-rotatory vestibular effects to decay. White noise was provided via 2 speakers (for each ear) attached to the chair to mask any auditory cues from the environment.

2.5. Posturography

Postural sway was assessed using a force platform for 60 s duration under four conditions: hard surface with eyes open (HO), hard surface with eyes closed (HC), soft surface with eyes open (SO), and soft surface with eyes closed (SC). Subjects were instructed to stand with their arms hanging loosely and to maintain their balance. SC condition is primarily vestibular dependent due to reduced proprioceptive (soft surface) and visual feedback (eyes closed); SC has also been shown to best differentiate in balance performance between TBI patients and healthy controls [5]. Root mean square (RMS) sway calculated using custom MATLAB scripts, during SC condition was thus chosen as the covariate for removing the confounding effect of balance from motion perception in neuroimaging analysis.

2.6. Vestibular agnosia classification

Vestibular perceptual thresholds from 37 healthy participants (Mean Perceptual Thresholds: 0.76 deg./s^2, SD = 0.42) were used to establish a normative range. We previously used a more conservative approach by classifying patients with having VA if their mean perceptual threshold (average of perceptual thresholds in right and left direction rotations) were above the mean + 3 standard deviation of the perceptual thresholds of healthy controls [5]. This criterion enhances specificity but at the cost of reduced sensitivity. We thus used a less conservative but arguably

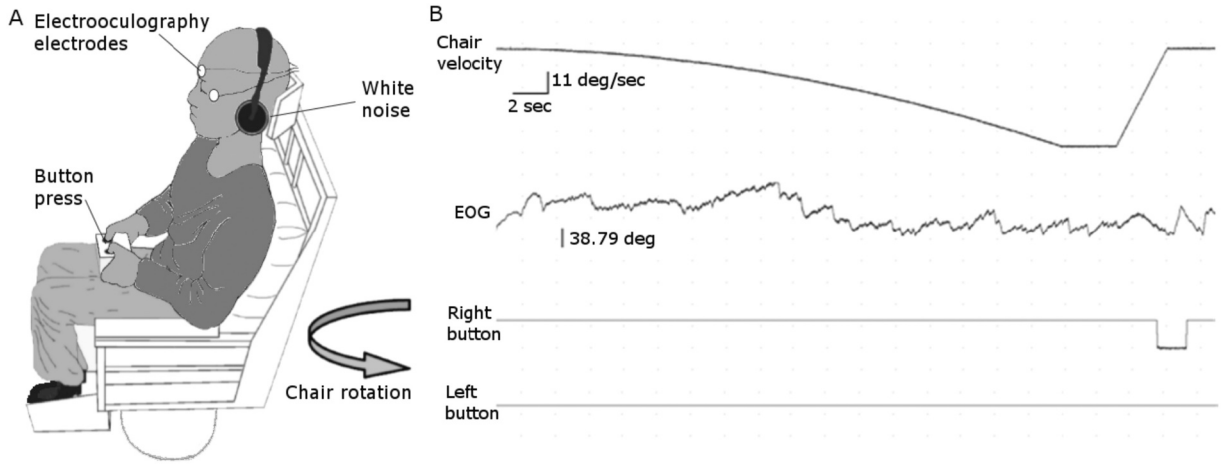

Fig. 1. Vestibular thresholds. Apparatus and methods. (A) Rotating Chair. (B) Representative raw traces of the signals during a chair rotation.

more objective approach for classification using all 76 participants (healthy: 37; TBI: 39) through k-means clustering. We identified 3 clusters (Fig. 2): i) cluster 1 was composed of subjects with normal perceptual thresholds (labeled as healthy controls and normal TBI in Fig. 2); ii) cluster 2 was composed of subjects with moderately high perceptual thresholds (labeled as healthy outliers and moderate VA TBI in Fig. 2), and iii) cluster 3 was composed of subjects with high perceptual thresholds (labeled as high VA TBI in Fig. 2). 19 TBI patients from cluster 2 and 3 with moderately high and high perceptual thresholds respectively (Mean Perceptual Thresholds: 4.20 deg./s^2, SD = 3.92), were classified as having vestibular agnosia (VA+) whereas 20 TBI patients (Mean Perceptual Thresholds: 0.85 deg./s^2, SD = 0.28) clustered with the healthy subjects in cluster 1 were considered patients without vestibular agnosia (VA-).

3. Neuroimaging

Historically, fMRI studies have assessed activity in grey matter [43] whereas fMRI activity within the white-matter was considered noise. However, recent evidence suggests that the BOLD signal in white matter has similar hemodynamic response characteristics as in grey matter [20] and the functional activity in underlying white-matter tracts maps along the direction of white-matter tracts [13,14]. Several studies have reported the presence of a white-matter functional architecture corresponding to resting state functional activity [28,35,47] as well as task related activity [27,28,38]. We thus performed neuroimaging analysis in grey- and white-matter regions separately using resting-state fMRI scans. After excluding 13 of 39 TBI patients due to different field of view scanning parameters (n = 12 of 39) and different TR time (n = 1 of 39), we were left with 26 TBI patients (11 VA+ and 15 VA-) whose data were included in the neuroimaging analysis.

3.1. Control group

Healthy control data was not used in the imaging analysis and were used only in supporting the classification of vestibular agnosia. Imaging analysis compared TBI patients without vestibular agnosia (VA-) to TBI patients with vestibular agnosia (VA+). Thus, we selected the VA- TBI patients as control group. Our rationale behind this was to minimize the TBI specific findings and only identify the regions associated with vestibular agnosia. Using healthy control group would result in numerous findings that would be associated with brain injury and not

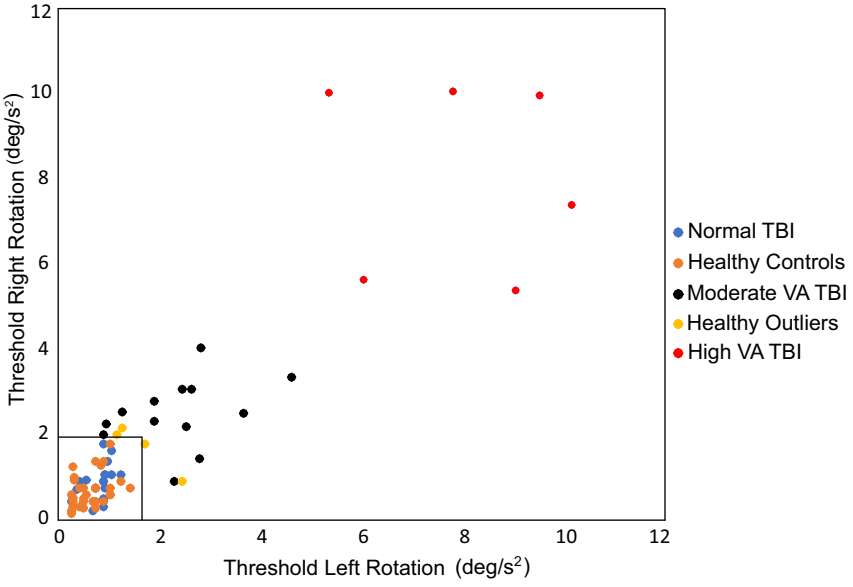

Fig. 2. K-means clustering with 3 clusters. K-mean clustering was performed on subjects' perceptual thresholds on right and left sides and three clusters were determined.

with vestibular agnosia per se, which is not the focus of this study. Thus, we used VA+ and VA- for imaging comparisons and performed stringent controls on imaging data for increasing the homogeneity between the two patient groups.

3.2. Patient group

The detailed demographics of the patients included in this study ($n = 26$) are listed in Table 1. There were no differences in the age of the two sub-groups (Mean ± SD: VA+ group: 43 ± 15.34 years; VA- group: 42.07 ± 13.61 years) confirmed via independent *t*-test assuming unequal variances ($t = 0.16$, $p > 0.05$). Also, we had more males ($n = 20$) than females ($n = 6$), however, chi-square test indicated no difference in gender in the two sub-groups of VA+ ($n = 4$ females) and VA- (n = 2 females) ($\chi^2 = 0.257$, p > 0.05).

Seven patients of n = 26 (3 vestibular agnosia (VA+) and 4 without vestibular agnosia (VA-)) performed the behavioural testing while they were on a medication. Four (1 VA+ and 3 VA-) of these 7 patients were also scanned while they were prescribed a neuroactive medication. We have reported the type of neuroactive medication of these patients in Table 2. Previous reports show no evidence of an effect of medication on the vestibular mediated self-motion perception [46,64] including a double-blind, randomized control, crossover study, which showed that Prochlorperazine has no effect upon any measure of nystagmic or perceptual vestibular function [46].

We evaluated the vigilance of patients to see if there were any differences between the two groups (VA+ and VA-). All patients performed a reaction time task in which mean reaction times were measured from stimulus onset to the time of the button press. For the patients included in this study, we found that there was no significant difference (t (19.853) = 0.846, $p = 0.408$) between the reaction times of the patients

Table 2
Patient medications.

Patient	Medication prescribed when behavioural testing performed	Medication prescribed when scanned
1	None	None
2	Levetiracetam	None
3	Levetiracetam	None
4	None	None
5	Levetiracetam	Levetiracetam
6	None	None
7	None	None
8	None	None
9	None	None
10	None	None
11	None	None
12	None	None
13	None	None
14	None	None
15	None	None
16	NA	NA
17	Levetiracetam	Levetiracetam
18	Sertraline	Sertraline
19	None	None
20	Prochlorperazine	None
21	None	None
22	None	None
23	None	None
24	None	None
25	None	None
26	Modafinil	Modafinil

NA: Missing information; None: No medication prescribed when laboratory testing/scan was performed.

Table 1
Patient demographics.

Pt	Gender: Age	GCS	MOI	Severity MAYO	Injury to lab testing (Days)	Injury to scan (Days)	DAI on MRI	Vestibular agnosia	CT brain lesions
1	M: 23	13	Assault	Mod-Sev	10	19	+	+	R Temporal pole & Occipital SDH, R Temporoparietal SAH, Frontal Contusions
2	F: 54	15	RTA	Mod-Sev	5	10	−	−	R Cerebral & Frontal SDH
3	F: 59	14	Fall	Mod-Sev	2	9	+	+	R Frontal Contusions, Contracoup L Anterior Temporal
4	M: 65	14	Fall	Mod-Sev	21	21	−	+	R Frontal & Parietotemporal SDH, L SAH
5	M: 37	14	RTA	Mod-Sev	11	11	+	+	None
6	F: 62	15	Fall	Mild-Prob	13	22	−	+	None
7	M: 40	15	Fall	Mod-Sev	4	13	−	−	R Parietal SAH
8	M: 58	15	Fall	Mod-Sev	6	13	+	−	L Frontal SAH
9	M: 42	15	RTA	Mod-Sev	7	16	+	+	L Frontal SAH, R Contracoup Temporo-occipital SAH, R SDH
10	M: 30	15	Fall	Mod-Sev	11	16	−	−	None
11	F: 60	15	Fall	Mod-Sev	4	12	−	−	L SAH & SDH, R Temporal Lobe Contusion, Bilateral Frontal SAH and SDH
12	M: 47	15	Fall	Mod-Sev	12	21	−	−	L SAH, L SDH
13	M: 49	14	Fall	Mod-Sev	19	25	−	+	Bifrontal and R Temporoparietal IPH, L SAH & SDH
14	M: 47	15	Fall	Mod-Sev	15	21	−	−	R Parietal SDH, Haemorrhagic Contusion L Inferior Temporal Pole
15	M: 24	8	Assault	Mod-Sev	20	26	+	−	R, L Temporal SDH, SAH
16	F: 40	13	Fall	Mod-Sev	33	33	+	−	L Temporoparietal SDH
17	M: 56	14	Fall	Mod-Sev	15	23	−	−	R Frontal SDH, L Tentorium SDH
18	M: 39	15	Fall	Mod-Sev	29	27	+	−	Bifrontal Contusions and SAH
19	M: 18	15	RTA	Mod-Sev	16	21	+	+	None
20	M: 34	3	Assault	Mod-Sev	28	41	−	+	R Temporal & L Occipital SDH
21	M: 48	14	Fall	Mod-Sev	14	31	−	+	Bifrontal SAH, SDH
22	M: 59	15	Fall	Mild-Prob	22	22	+	−	None
23	M: 36	12	RTA	Mod-Sev	77	77	−	+	L SDH, SAH (Right parietotemporal injury)
24	F: 20	15	RTA	Mod-Sev	24	24	+	−	R Parietal, R Anterior Temporal SDH, L Parietal and R Frontal SAH
25	M: 29	3	Fall	Mod-Sev	27	28	−	−	L Frontal and Temporal SAH
26	M: 28	14	RTA	Mod-Sev	7	12	+	−	None

+/−: present/absent; DAI: diffuse axonal injury; GCS: Glasgow Coma Scale (in Accident & Emergency); L: left; Mod/Sev/Prob: moderate/severe/probable; MOI: mechanism of injury; R: right; RTA: road traffic accident; SAH: subarachnoid haemorrhage; SDH: subdural haemorrhage; IPH: intraparenchymal haemorrhage.

with vestibular agnosia (VA+) and those without (VA-), confirmed via Welch's independent t-test (without equal variance assumption). Additionally, a Bayesian independent t-test showed a bayes factor of $BF_{10} = 0.481$, which is negligible evidence for the hypothesis that the mean reaction times of two groups are different. Thus, both subgroups of patients performed the test equally well showing no effect of delayed response due to inattention or sedatives.

We also performed Welch's independent *t*-tests comparing the difference in "Days from injury to lab testing" and "Days from injury to scan" between the subgroups VA+ and VA- (reported in Table 1). We found no differences in the days from injury to lab testing of the two subgroups ($t(13.408) = 0.533$, $p = 0.533$) with bayes factor of $BF_{10} = 0.441$, nor was there any difference in days from injury to scan ($t(12.038) = 1.098$, $p = 0.294$) with bayes factor of $BF_{10} = 0.641$, suggesting no evidence of difference in time to test or scan from the injury. Note that none of these tests were corrected for multiple comparisons as to show that there was no or minimal heterogeneity in the sample of patients.

3.3. Image acquisition

Structural and functional MRI images were acquired using a 3 T Siemens Verio (Siemens) scanner, using a 32-channel head coil. The scanning protocol included: (i) 3D T1-weighted images acquired using MPRAGE sequence (image matrix: 256 × 256; voxel size: 1 × 1; Slices: 160; field of view: 256 × 256 mm; slice thickness: 1 mm; TR = 2300 ms; TE: 2.98 ms); (ii) T2*-weighted images sensitive to blood oxygenation level dependent (BOLD) signal for resting state fMRI (image matrix: 64 × 64; voxel size: 3 × 3 × 3 mm^3; Slices: 35; field of view: 192 × 192 mm; flip angle: 80°; slice thickness: 3 mm; TR = 2000 ms; TE: 30 ms; volumes = 300; scan time = 10 min); and (iii) FLAIR scans (voxel size: 1 × 1 mm; Slices: 160; field of view: 250 mm; slice thickness: 1 mm; TR = 5000 ms; TE: 395 ms). Subjects were instructed to keep their eyes closed, stay awake, and to try not to think of anything.

3.4. Preprocessing

Data were preprocessed using the CONN Toolbox [60] based on Statistical Parametric Mapping (SPM12; http://www.fil.ion.ucl.ac.uk/spm/). Preprocessing steps were as follows. (1) Realignment to mean functional image, unwarping, and susceptibility distortion correction. (2) Slice timing correction. (3) Functional outlier detection using ART (artifact detection toolbox), with scans exceeding a conservative framewise displacement threshold of 0.5 mm labeled as outliers [48]. (4) Structural segmentation and normalization. (5) Indirect functional normalization using deformation fields estimated from structural normalization. (6) Group analysis space masks: two analysis space masks were created: 1) grey-matter (GM) specific; 2) white-matter (WM) specific. The individuals' segmented masks were binarized (GM: $p > 0.2$; WM: $p > 0.8$) and then averaged across subjects. To control for partial volume effects, the average masks were then binarized at $p > 0.7$ for GM specific mask and $p > 0.9$ for WM specific mask creation. (7) Smoothing (6 mm FWHM) was performed within the grey- and white-matter using GM and WM masks separately. (8) Subsequently, denoising was performed in which six motion regressors (3 translational and 3 angular motion), their temporal derivatives, mean cerebrospinal fluid, and outlier scans identified by ART toolbox were regressed out. (9) Data were then band-pass filtered with a frequency range of 0.008–0.1 Hz. White matter activity and the global signal were not regressed out since white-matter activity was the signal of interest whereas the global signal regression is known to introduce negative correlations [40]. The mean motion for the VA+ group (Mean ± SD: 0.15 ± 0.05) and for the VA- group (Mean ± SD: 0.17 ± 0.06) was not different from each other when compared statistically using two-sided independent *t*-test and assuming unequal variances ($p > 0.05$).

3.4.1. Lesion mapping

For lesion mapping, all intrinsic brain lesions were included whereas extrinsic lesions (e.g. a subdural- haematoma) were not masked as lesions. We used a lesion prediction algorithm (LPA) in the Lesion Segmentation Toolbox (v3.0.0) (http://www.applied-statistics.de/lst.html) to segment white-matter lesions in a fully automated way using FLAIR scans. Lesion masks were then further inspected visually for any structural damage using T1-contrast scans. Any lesions identified in T1 scans were mapped in a semi-automated way using MRIcron software [50]. The volume (in millilitres) of the lesion masks of the individuals was then estimated in MRIcron. The mean lesion volume was higher in the VA+ group (Mean ± SD: 17.70 ± 17.23) compared to VA- group (Mean ± SD: 7.07 ± 7.70), however, a two-sided independent t-test (assuming unequal variances) showed that the lesion volumes were not significantly different ($p > 0.05$). We also performed a point-biserial correlation to confirm if there was a correlation between lesion volume and vestibular agnosia, but we found no significant correlation (Pearson's $r = 0.314$, $p > 0.05$).

To increase the homogeneity between the two patient groups and to remove any effects that can be explained due to brain lesions, we used this estimated lesion volume as a confound regressor at group-level analysis.

3.4.2. Control for partial volume effects

We used extremely stringent thresholds for creating group masks to control for any partial volume effects. White matter masks were binarized at $p > 0.8$ (compared to default of $p > 0.5$). Additionally, after generating the average white-matter group mask, we binarized the mask at an extremely conservative threshold of $p > 0.9$. Similarly, for grey matter we used $p > 0.2$ threshold for generating binary mask and after generating the average grey-matter group mask, we binarized it at a conservative $p > 0.7$. This kind of stringent control for group masks is not often performed and is likely to improve specificity of the analysis and the homogeneity of the two patient groups.

3.4.3. Control for volume differences

To ensure that the group functional differences were not due to the volumetric differences between the patient groups, we estimated grey- and white-matter volumes of individuals by performing voxel based morphometry (VBM) analysis using CAT12 software [22]. These volume estimates were then used as confound regressors in group level analysis.

3.5. Second-level analysis

A group level analysis was performed to determine the differences between VA+ ($n = 11$) TBI patients and VA- ($n = 15$) TBI patients.

3.5.1. Confound regressors

RMS sway and lesion volume were added as covariates in group-analysis to remove the effects explained by balance and extent of injury. In addition, volume regressors were also added to control for tissue atrophy as a result of injury or volumetric differences between subjects. Grey matter volume was added as a covariate in GM specific analysis whereas white matter volume was added in WM specific analysis.

3.5.2. Independent component analysis

Group independent component analysis (ICA) was performed to assess the intra-network resting state differences between VA+ and VA- groups using Fast ICA algorithm in CONN toolbox [60]. The optimal number of the independent components (ICs) were estimated in the GIFT toolbox (https://trendscenter.org/software/) using a modified minimum description length algorithm (MDL). The optimal number of ICs for GM specific analysis were found to be 38 and 10 for WM specific analysis. In grey-matter, however, we estimated 15 ICs to reduce overfitting and sub-division of ICs, and to avoid statistical evaluation of

multiple ICs.

3.5.3. Region of interest analysis

A ROI Analysis was used to assess the inter-network resting state differences between VA+ and VA- groups. A ROI-to-ROI analysis assesses the connectivity between all pairs of ROIs, using a ROI-ROI matrix where each ROI is assumed to have a functional connection with all other ROIs. The functional connections from each ROI to all other ROIs are then compared statistically between the two groups (VA+ and VA-) and corrected for multiple comparisons.

For GM specific ROI analyses, we used an atlas of resting state networks available with CONN toolbox, determined using Human Connectome Project dataset of 497 subjects. We did not select specific ROIs, but rather used all available ROIs (32 ROIs) for the ROI-ROI analysis.

Since there are no established white-matter resting-state networks, white matter regions from the ICBM-DTI-81 atlas [39,44] were used as ROIs. We used all 50 regions for the ROI-ROI analysis. Both of these are equivalent to a whole brain analysis but at a network level instead of voxel level.

4. Statistical analysis

The assumptions of Gaussian random field theory (RFT) are required for whole brain analysis [41] and thus parametric RFT statistics are not applicable for GM or WM specific analysis. Permutation statistics (non-parametric), however, does not require Gaussian RFT assumptions [66]. Moreover, the choice of cluster height threshold (either $p < 0.01$ or $p < 0.001$) has no impact on false positive rate when using permutation statistics for whole brain analysis as demonstrated in a previous study [17].

Thus, all group level differences in ICA and seed-based analysis were evaluated using permutation statistics [4] and cluster mass FWE (family-wise error) correction for multiple comparisons. Cluster height threshold for all grey-matter specific analysis was selected as $p < 0.001$ and for all white-matter specific analysis as $p < 0.01$, as choice of height thresholds reveal different architecture in grey- and white-matter. For both GM and WM specific ROI analysis, ROI level FWE mass correction for multiple correction was used.

The findings are reported as MNI coordinates (MNI: x, y, z). For discussion purposes, findings from previous studies, if in Talairach space, were converted to MNI using the Yale bioimage suite [33].

4.1. Sample size

Effect sizes in the TBI cohort are often large such that the differences between patients are easily visible to the naked eye during the clinical assessments. In our cohort, vestibular agnosia was not only apparent during clinical assessment [5], the difference is also very large when comparing objectively assessed perceptual thresholds of VA+ (4.20 deg./s^2) vs VA- (0.85 deg./s^2) with an effect size of Cohen's d = 1.2. Considering that this is the first study looking at the functional brain correlates of VA, it was not possible to appropriately power the study using previous data. However, from previous studies, it is evident that even small sample sizes in TBI cohorts, such as 11 TBI with post-traumatic amnesia (PTA) vs 8 TBI without PTA [9], 12 TBI with post-concussion syndrome (PCS) vs 16 TBI without PCS [57], and 8 concussed TBI vs 11 healthy [67] are adequate to identify functional brain differences with decent effect sizes (Hedge's g up to 1.8). Similarly, functional brain differences in a group of 7 vs 7 TBI patients with impaired or normal balance, which is also mediated by vestibular

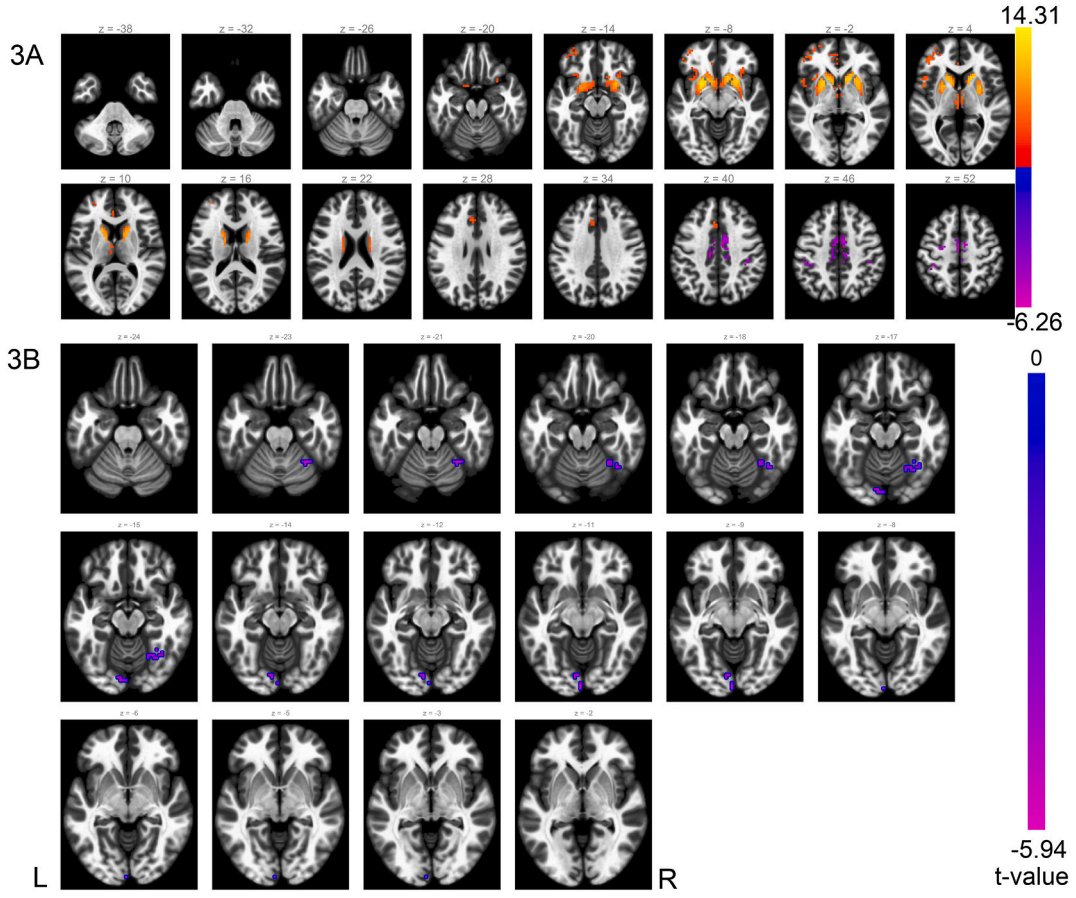

Fig. 3. GM Specific ICA. (A) Independent component 3. (B) Group comparison between VA+ and VA- patients showing decreased functional connectivity in two clusters composed of right temporo-occipital fusiform cortex and left lingual gyrus. *(colorbar represent t-values; voxel level $p < 0.001$ & cluster level $p < 0.05$).*

networks, have also recently been identified [63]. It follows that given the stringent controls in the imaging analysis, the large clinical and objective effect size, and a sample size comparable to other similar rsfMRI studies in TBI, the likelihood of any false positives in our data is low. Since no previous study has looked at vestibular agnosia, our study will allow future sample size calculations for studies evaluating vestibular agnosia.

5. Results

5.1. Independent component analysis

5.1.1. GM specific independent component analysis

To identify differences within specific grey-matter resting state networks, we looked at independent components. In grey-matter specific ICA, group differences were identified in IC-3, a striatal resting-state network largely composed of caudate and putamen, and also containing voxels from bilateral supplementary motor area (SMA), anterior cingulate cortex, left-frontal pole, bilateral thalamus, and bilateral pre- and post-central gyrus (Fig. 3A showing group independent component estimated via group ICA). We found two clusters in which VA+ group compared to VA- group had decreased functional connectivity. First cluster (MNI coordinates: +30, −51, −21) was composed of 22 voxels with 16 voxels at right temporo-occipital fusiform cortex and 6 voxels comprising right cerebellum lobule VI, shown in Fig. 3B, slice z = −20 (t(21) = −6.37, pFWE <0.05). Second cluster (MNI coordinates: −03, −90, −09) was composed of 17 voxels with 13 voxels at left lingual gyrus, 3 voxels comprising left occipital pole, and 1 voxel covering left occipital fusiform gyrus, shown in Fig. 3B, slices z = −14 to z = −8 (t(21) = −6.12, pFWE <0.05).

Additionally, group differences were also identified in IC-12, a lateral visual resting state-network largely composed of regions from bilateral superior and inferior lateral occipital cortex and also included clusters from bilateral insular cortex, bilateral post-central gyrus, bilateral supramarginal gyrus, bilateral parahippocampal region, left hippocampus, and right lingual gyrus (Fig. 4A showing group independent component estimated via group ICA). We found a cluster in which VA+ group compared to VA- group had decreased functional connectivity. The cluster (MNI coordinates: +24, −54, −09) was composed of 19 voxels with 10 voxels in right lingual gyrus, 6 in right temporo-occipital fusiform cortex, 2 in right cerebellum lobule VI, and 1 voxel overlapping right cerebellum lobules IV, V. The regions are shown in Fig. 4B, slices z = −20 to z = −8 (t(21) = −5.76, pFWE <0.05).

The findings in Figs. 3 and 4 are displayed on a representative brain; for accurate anatomical locations we refer the reader to MNI coordinates of cluster centres.

5.1.2. WM specific independent component analysis

To identify differences within specific networks, we looked at independent components. We found no significant differences in functional connectivity between VA+ and VA- group in white-matter specific ICA.

5.2. Regions of interest analysis

5.2.1. GM specific regions of interest analysis

For between resting-state network differences, we performed grey-

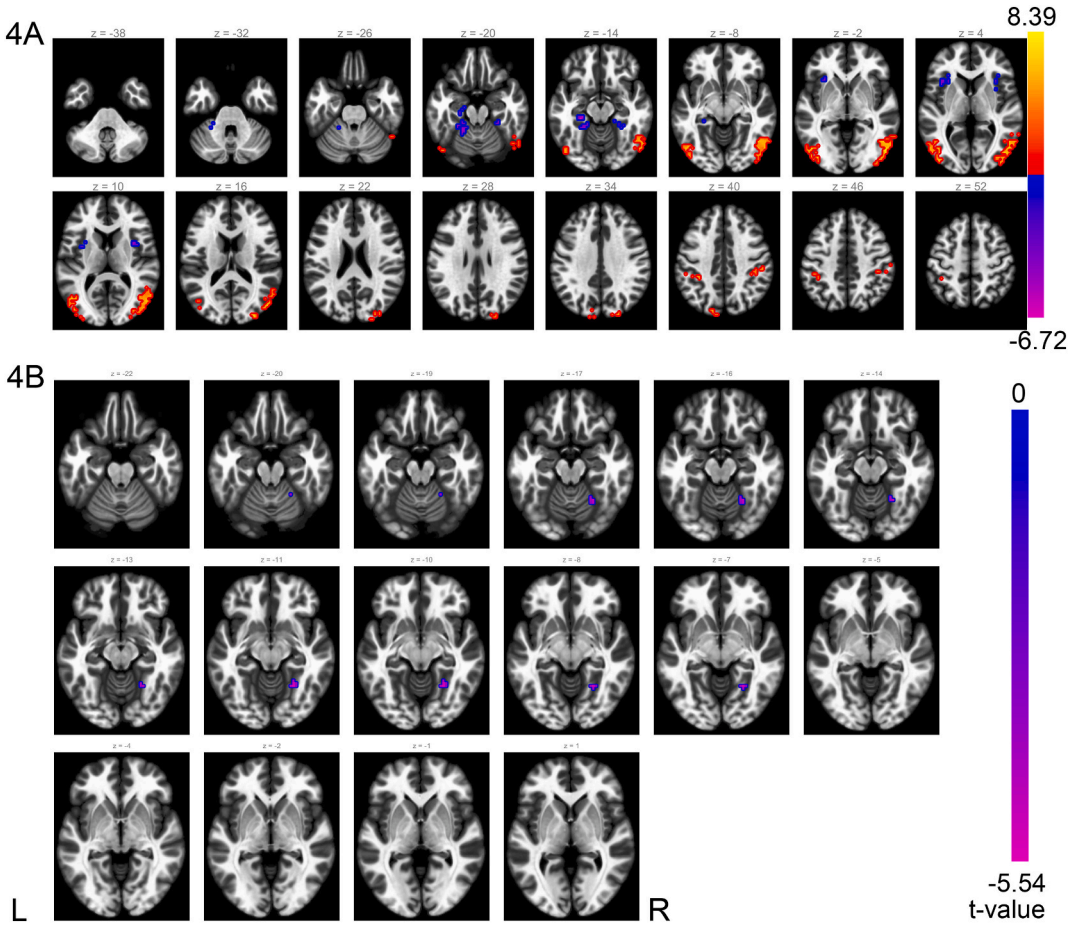

Fig. 4. GM Specific ICA. (A) Independent component 12. (B) Group comparison between VA+ and VA- patients showing showing decreased functional connectivity in a cluster largely composed of right lingual gyrus and right temporo-occipital fusiform cortex (slices z = −20 to z = −8). *(colorbar represent t-values; voxel level p < 0.001 & cluster level p < 0.05).*

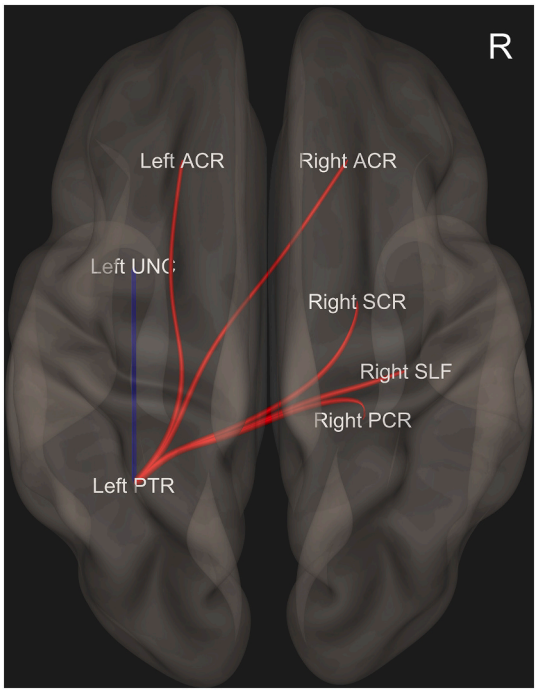

Fig. 5. WM Specific ROI Analysis. 50 white-matter regions from ICBM-DTI-81 atlas were compared for differences in functional connectivity between VA+ and VA- groups. A difference in functional connectivity was found in a group of ROI connections including left and right anterior corona radiata (ACR), right superior corona radiata (SCR), right superior longitudinal fasciculus (SLF), right posterior corona radiata (PCR), left uncinate fasciculus (UNC), and left posterior thalamic radiation (PTR). Red represents the group of connections that have higher functional connectivity in VA+ (vs VA-) and blue represents the group of connections that have lower functional connectivity in VA+ (vs VA-). (evaluated at $p < 0.01$).

matter ROI-ROI analysis. We found no significant differences in functional connectivity between VA+ and VA- group in grey-matter specific ROI-ROI analysis using 32 seed ROIs.

5.2.2. *WM specific regions of interest analysis*

For differences between white-matter networks, we looked at white-matter ROI-ROI differences using 50 white-matter ROIs. WM specific ROI analysis resulted in a single group of 6 connections (Fig. 5), (ROI mass = 101.80, pFWE <0.05). This group was composed of: left and right anterior corona radiata (ACR), right superior corona radiata (SCR), right superior longitudinal fasciculus (SLF), right posterior corona radiata (PCR), left uncinate fasciculus (UNC), and left posterior thalamic radiation (PTR). The VA+ group in all of these ROIs had increased functional connectivity with the left PTR except the left UNC, which had decreased functional connectivity with the left PTR.

6. Discussion

Using DTI imaging, we previously identified that VA was linked to imbalance via damage to the right ILF [5], however, we were unable to identify the brain regions specifically explaining VA. Given our a priori hypothesis that vestibular-motion perception is mediated by multiple brain networks, we used resting-state fMRI to identify the functional brain networks linked to vestibular agnosia. We found that vestibular agnosia is linked to: (i) altered functional connectivity in a bilateral white-matter network; and (ii) decreased functional connectivity in bilateral lingual gyri (V3v/V4) and temporo-occipital regions.

6.1. *Vestibular agnosia and white-matter fMRI*

Using white-matter ROI analysis, we found that vestibular agnosia was linked to a bilateral and anterior-posterior network (Fig. 5) composed of left and right anterior corona radiata (ACR), right superior corona radiata (SCR), right superior longitudinal fasciculus (SLF), right posterior corona radiata (PCR), left uncinate fasciculus (UNC), and left posterior thalamic radiation (PTR). However, we did not find any differences between VA+ or VA- groups when looking at white-matter ICA.

Abnormal DTI parameters in the same network of white-matter tracts as we found (shown in Fig. 5), has previously been reported to be linked with impaired balance in elderly patients with small vessel disease [51]; although this study did not assess patients' ability to perceive self-motion. Notably however, there are multiple accounts of VA in patients with small vessel disease and impaired balance [7,29,52], thus suggesting the involvement of overlapping albeit distinct networks, mediating multiple vestibular functions.

Electro-cortical stimulation to the right SLF [58] and left SLF [30] induces sensations of self-motion in the yaw plane indicating a bilateral coding of self-motion sensations via SLF. We also previously found that a bilateral network mainly composed of the SLF was associated with the duration of vestibular self-motion sensation following a whole body yaw rotational acceleration ('stopping responses') in the dark in healthy subjects [42]. Thus, our finding of right SLF is in line with previous reports and complements the role of right SLF in self-motion processing specifically in yaw-plane.

The left posterior thalamic radiation (PTR), bilateral superior corona radiata (SCR), and right posterior corona radiata (PCR) have been linked with impaired balance in mild TBI and elderly adults [23,51]. Since we controlled for the variance explained by balance in our resting-state analysis, our results suggest that these networks also have a unique functional role in mediating yaw-plane perception of self-motion.

While we did not find any differences in white-matter ICA, in a previous version of this analysis in which we completely removed individuals' brain lesions from the group analysis mask (even though all lesions were heterogenous), we found a large cluster in right SLF with increased functional connectivity in the VA+ subjects [24]. However, since lesions were heterogenous, we decided against this aggressive control for lesions and included those regions in the group analysis mask and instead used the lesion volume estimate as confound.

The absence of any significant group differences (VA+ vs VA-) in white-matter ICA is not contradictory to ROI-ROI analysis. ROI analysis was performed to assess if functional link between multiple resting-state networks is altered in VA+ compared to VA- whereas ICA assessed if functional connectivity within a particular resting-state network is altered in VA+ compared to VA-. The absence of ROI-ROI difference could reflect that individual white-matter resting-state networks are not altered in vestibular agnosia, but insufficient power could also be the reason of absence of these findings.

6.2. *Vestibular agnosia and grey-matter fMRI*

Using ICA we found decreased functional connectivity in two independent components (ICs) in the VA+ group; one IC containing functional differences composed of the left lingual gyrus and another comprising functional differences within the same regions on right hemisphere. In addition, both ICs also contained right temporo-occipital fusiform cortex. Given our previous report of ILF white matter microstructural disruption in VA patients [5], and the known connectivity of the ILF linking the temporal and lingual gyri [34,45], this pattern of findings was perhaps predictable.

6.2.1. *Role of lingual gyrus in self-motion processing*

The lingual gyrus appears to be an important vestibular processing hub that is also involved in visuo-vestibular motion processing [12,49,69]. Indeed electrocortical stimulation of the lingual gyrus

evoked a yaw-plane self-motion sensation [30]. Hence, in addition to previous data implicating the lingual gyrus in motion processing, our data further suggest that a right hemisphere network involving the lingual gyrus and mid-temporal regions connected via the right ILF, is involved in yaw-plane self-motion processing. However, it is important to note that in our findings, the coordinates of cluster centres (MNI: 30, −51, −21) and (MNI: 24, −54, −09) were more anterior in comparison to [30] MNI: (26, −71, +5) as well as [12] MNI: (24, −82, −8). Thus, the role of the lingual gyrus in processing of yaw-plane self-motion needs to be further investigated.

6.2.2. Role of temporo-occipital fusiform cortex in self-motion processing

In addition, our findings also contained right temporo-occipital fusiform cortex, which is also a part of higher order visual regions that are involved in motion processing. Previous reports show that the occipital fusiform gyrus (V4) [12] and temporo-occipital junction (V5/MT) are linked to BOLD activations during visual motion stimuli [71]. V5/MT is reported to show reduced BOLD activation during illusory self-motion sensation [71], however, the fusiform gyrus (V4) is reported to show BOLD increases [12] and decreases [3] in response to vestibular stimulation. While human MT complex has been shown to be modulated by vestibular stimulation [1,69], it is possible that activation of human MT complex is due to the activation of MST, since another study has shown strong vestibular modulation of MST with no effect in MT [56]. It is however important to note that the human MT complex is located more laterally (MNI Coordinates: (43, −63, −2) [1]; (39, −60, −8) [6]) compared to our finding of right temporo-occipital fusiform cortex (MNI Coordinates: (30, −51, −21)), which is located more medially (Fig. 3B).

A recent study in patients with bilateral vestibulopathy [25], using galvanic vestibular stimulation and putative vestibular regions as seed ROIs (Parietal operculum (OP1 and OP4) and posterior insula (Ig2)), reported a difference in connectivity of the seeds with the fusiform gyrus (MNI: (24, −54, −15) & (21, −54, −15)) in the patients compared to healthy. Notably the cluster centres of these findings are closer to the cluster centres we report in this study (MNI Coordinates = IC3: (30, −51, −21) & IC12: (24, −54, −09)). While we cannot comment on the structural connectivity or the vestibular inputs to the temporo-occipital fusiform cortex, the clusters with functional connectivity differences in our study are similar to those reported previously [25] suggesting its specific involvement in yaw-plane self-motion processing. However, further investigation to establish causal and structural link of the fusiform region in yaw-plane self-motion perception is required.

6.2.3. Regions linked to visual and vestibular self-motion processing

Note that findings reported in our study are specific to impaired yaw-plane self-motion sensation. Galvanic vestibular stimulation (GVS) elicits head-centric roll-plane sensations [25,56] although occasionally may elicit yaw sensations [56]. The visual motion processing areas, which include human middle temporal complex (hMT+) [1], human medial superior temporal area (hMST) [56], cingulate sulcus visual (CSv) [1,56], posterior insular cortex (PIC) [1,37], ventral intraparietal region (VIP) [1,56], and area V6 [1] are also activated in response to GVS in the dark (i.e. without visual input) suggesting their link to vestibular self-motion sensation. Area V6 and VIP have been reported to have more sensitivity for pitch plane stimulation [1], which is congruent with the observation that Smith and colleagues [56] did not observe strong activations of these regions in response to GVS eliciting roll-plane self-motion sensation. Whereas hMT+, CSv, and PIC show equivalent sensitivity to both pitch or roll type of stimulus [1]. Since these regions have not been specifically tested for yaw-plane sensations, it could explain the absence of these regions in our findings. However, we cannot objectively address the role of the above mentioned regions in self-motion perception based on our findings.

6.2.4. Sensory integration and vestibular agnosia

Sensory integration is often considered to be a function of frontal brain regions such as regions in the salience resting state network e.g. rostral prefrontal cortex (RPFC) [59]. One proposal posits an accumulation of evidence, with perceptual 'ignition' ocurring following sufficient accumulated evidence [10,11]. Thus, we suggest that VA could arise either by a sensory integration disruption or by perceptual ignition failure. Notably, a previous version of our data suggested involvement of the salience resting state network in mediating VA [24].

6.2.5. Role of cerebellum in self-motion processing

Lastly, in both our ICA findings, the clusters also included some voxels from cerebellum lobule VI (IC-3: 6 voxels; IC-12: 2 voxels), which has previously been shown to have greater fMRI activation in response to vestibular stimulation but is also activated during simultaneous visuo-vestibular stimulation [12], however, the interpretation of these findings is limited by the small number of voxels lying in these regions.

6.2.6. Absence of grey-matter differences in ROI analysis

While we found group differences (VA+ vs VA-) in grey-matter ICA, we did not find any group differences in grey-matter ROI-ROI analysis. The absence of ROI-ROI differences in grey-matter could reflect that VA+ and VA- had no differences in functional association between multiple resting-state networks. However, the absence of the group differences is not contradictory to our ICA findings, since ICA assessed whether a particular resting-state network was altered in VA+ compared to VA-, as opposed to the ROI-ROI analysis, which assessed if the functional link between multiple resting-state networks is altered in VA+ compared to VA-.

7. Limitations

Vestibular agnosia (VA), while clinically apparent, can currently only be objectively identified via self-motion perception testing in a rotatory-chair in dark. Moreover, VA is classified based on a continuous parameter i.e. sensory thresholds of motion perception, and thus mild or borderline cases may or may not be classified as having VA. Another limitation of the study is the relatively small sample size. This was partly due to a limited number of vestibular agnosia patients, which is unavoidable considering that prevalence of VA is not yet known, and patients are classified post-hoc based on objective laboratory testing. However, our sample size is comparable to previous fMRI studies in traumatic brain injury [9,57,63].

VA is known to impact frail elderly fallers [7,29,52,53,70] and neurodegeneration patients [65], however an advantage of our patient group was their relative young age and good premorbid health excluding incipient neurodegenerative disease (given our stringent exclusion criteria), hence the findings reported herein were overwhelmingly related to the acute TBI and not to other chronic underlying disease.

In addition to controlling for TBI specific findings, we performed stringent controls of imaging data to increase between group homogeneity of TBI patients. Since we did not find any functional differences in default-mode network (one of the resting state networks commonly effected in TBI), we think that our findings are non-TBI specific.

One limitation of this study is lack of a priori control for the effects of medication. Due to the acute prospective nature of our study, some patients performed the behavioural testing and were scanned while they were prescribed neuroactive medications. While we found no differences in vigilance of our study subgroups, we cannot objectively comment if the behavioural measures or scans were affected in our patients due to neuroactive medications.

8. Conclusion

Our data provide the first evidence linking resting-state functional networks to vestibular agnosia – impaired self-motion perception in yaw-plane. More specifically, we show that yaw-plane self-motion

perception is mediated via bihemispheric brain networks, composed of posterior vestibular regions involved in sensory processing, higher order posterior regions involved in perceptual ignition, and possible involvement of anterior regions associated with sensory integration.

Funding

The Medical Research Council (MRC) (MR/P006493/1). The Imperial Health Charity, The NIHR Imperial Biomedical Research Centre, NIHR Clinical Doctoral Research Fellowship (R. Smith - ICA-CDRF-2017-03-070), The US Department of Defense - Congressionally Directed Medical Research Program (CDMRP), The Jon Moulton Charity Trust.

Data and code availability statements

Raw data that support the findings of this study are available from the principal investigator, upon reasonable request. The request would require a formal data sharing agreement, approval from the requesting researcher's local ethics committee, a formal project outline, and discussion regarding authorship on any research output from the shared data if applicable.

CRediT authorship contribution statement

Zaeem Hadi: Investigation, Methodology, Software, Formal analysis, Visualization, Writing – original draft. **Mohammad Mahmud:** Investigation, Methodology, Writing – review & editing. **Yuscah Pondeca:** Investigation, Methodology, Writing – review & editing. **Elena Calzolari:** Investigation, Methodology, Writing – review & editing. **Mariya Chepisheva:** Investigation, Writing – review & editing. **Rebecca M. Smith:** Investigation, Methodology, Writing – review & editing. **Heiko M. Rust:** Investigation, Methodology, Writing – review & editing. **David J. Sharp:** Supervision, Writing – review & editing. **Barry M. Seemungal:** Conceptualization, Investigation, Project administration, Funding acquisition, Resources, Supervision, Writing – review & editing.

Declaration of Competing Interest

The authors declare that they have no conflict of interest.

Acknowledgments

We would like to thank our patient and healthy volunteers for their participation and for helping us improve the traumatic brain injury patients' care. We are also grateful to the major trauma ward teams at St Mary's Hospital and King's College Hospital London for their help with recruitment and assessment. We are also very grateful to The Imperial Health Charity who provided important kickstarter funding that enabled us to obtain research council funding for this project.

References

[1] F. Aedo-Jury, B.R. Cottereau, S. Celebrini, A. Séverac Cauquil, Antero-posterior vs. lateral vestibular input processing in human visual cortex, Front. Integr. Neurosci. 14 (2020) 43, https://doi.org/10.3389/FNINT.2020.00043/BIBTEX.

[3] S. Bense, T. Stephan, T.A. Yousry, T. Brandt, M. Dieterich, Multisensory cortical signal increases and decreases during vestibular galvanic stimulation (fMRI), J. Neurophysiol. 85 (2) (2001) 886–899, https://doi.org/10.1152/JN.2001.85.2.886/ASSET/IMAGES/LARGE/9K0211494006.JPEG.

[4] E.T. Bullmore, J. Suckling, S. Overmeyer, S. Rabe-Hesketh, E. Taylor, M. J. Brammer, Global, voxel, and cluster tests, by theory and permutation, for a difference between two groups of structural mr images of the brain, IEEE Trans. Med. Imaging 18 (1) (1999) 32–42, https://doi.org/10.1109/42.750253.

[5] E. Calzolari, M. Chepisheva, R.M. Smith, M. Mahmud, P.J. Hellyer, V. Tahtis, Q. Arshad, A. Jolly, M. Wilson, H. Rust, D.J. Sharp, B.M. Seemungal, Vestibular agnosia in traumatic brain injury and its link to imbalance, Brain J. Neurol. 144 (1) (2021) 128–143, https://doi.org/10.1093/brain/awaa386.

[6] V. Cardin, A.T. Smith, Sensitivity of human visual and vestibular cortical regions to Egomotion-compatible visual stimulation, Cereb. Cortex 20 (8) (2010) 1964–1973, https://doi.org/10.1093/CERCOR/BHP268.

[7] E. Chiarovano, P.P. Vidal, C. Magnani, G. Lamas, I.S. Curthoys, C. de Waele, Absence of rotation perception during warm water caloric irrigation in some seniors with postural instability, Front. Neurol. 7 (JAN) (2016), https://doi.org/10.3389/fneur.2016.00004.

[8] K.E. Cullen, Vestibular processing during natural self-motion: implications for perception and action, Nat. Rev. Neurosci. 20 (6) (2019) 346, https://doi.org/10.1038/S41583-019-0153-1.

[9] S. De Simoni, P.J. Grover, P.O. Jenkins, L. Honeyfield, R.A. Quest, E. Ross, G. Scott, M.H. Wilson, P. Majewska, A.D. Waldman, M.C. Patel, D.J. Sharp, Disconnection between the default mode network and medial temporal lobes in post-traumatic amnesia, Brain 139 (12) (2016) 3137, https://doi.org/10.1093/BRAIN/AWW241.

[10] A. Del Cul, S. Baillet, S. Dehaene, Brain dynamics underlying the nonlinear threshold for access to consciousness, PLoS Biol. 5 (10) (2007) 2408–2423, https://doi.org/10.1371/journal.pbio.0050260.

[11] A. Del Cul, S. Dehaene, P. Reyes, E. Bravo, A. Slachevsky, Causal role of prefrontal cortex in the threshold for access to consciousness, Brain 132 (9) (2009) 2531–2540, https://doi.org/10.1093/brain/awp111.

[12] H.M. Della-Justina, H.R. Gamba, K. Lukasova, M.P. Nucci-da-Silva, A.M. Winkler, E. Amaro, Interaction of brain areas of visual and vestibular simultaneous activity with fMRI, Exp. Brain Res. 233 (1) (2014) 237–252, https://doi.org/10.1007/s00221-014-4107-6.

[13] Z. Ding, A.T. Newton, R. Xu, A.W. Anderson, V.L. Morgan, J.C. Gore, Spatio-temporal correlation tensors reveal functional structure in human brain, PLoS One 8 (12) (2013) 82107, https://doi.org/10.1371/journal.pone.0082107.

[14] Z. Ding, R. Xu, S.K. Bailey, T.L. Wu, V.L. Morgan, L.E. Cutting, A.W. Anderson, J. C. Gore, Visualizing functional pathways in the human brain using correlation tensors and magnetic resonance imaging, Magn. Reson. Imaging 34 (1) (2016) 8–17, https://doi.org/10.1016/j.mri.2015.10.003.

[15] N.M. Dotson, R.F. Salazar, C.M. Gray, Frontoparietal correlation dynamics reveal interplay between integration and segregation during visual working memory, J. Neurosci. 34 (41) (2014) 13600–13613, https://doi.org/10.1523/JNEUROSCI.1961-14.2014.

[16] A. Dovern, G.R. Fink, A.C.B. Fromme, A.M. Wohlschläger, P.H. Weiss, V. Riedl, Intrinsic network connectivity reflects consistency of synesthetic experiences, J. Neurosci. 32 (22) (2012) 7614–7621, https://doi.org/10.1523/JNEUROSCI.5401-11.2012.

[17] A. Eklund, H. Knutsson, T.E. Nichols, Cluster failure revisited: impact of first level design and physiological noise on cluster false positive rates, Hum. Brain Mapp. 40 (7) (2019) 2017–2032, https://doi.org/10.1002/hbm.24350.

[18] E.F. Ester, D.W. Sutterer, J.T. Serences, E. Awh, Feature-selective attentional modulations in human Frontoparietal cortex, J. Neurosci. 36 (31) (2016) 8188–8199, https://doi.org/10.1523/JNEUROSCI.3935-15.2016.

[19] I.C. Fiebelkorn, M.A. Pinsk, S. Kastner, A dynamic interplay within the Frontoparietal network underlies rhythmic spatial attention, Neuron 99 (4) (2018) 842–853.e8, https://doi.org/10.1016/J.NEURON.2018.07.038.

[20] L.M. Fraser, M.T. Stevens, S.D. Beyea, R.C.N. D'Arcy, White versus gray matter: fMRI hemodynamic responses show similar characteristics, but differ in peak amplitude, BMC Neurosci. 13 (1) (2012) 91, https://doi.org/10.1186/1471-2202-13-91.

[21] G. Galati, G. Committeri, J.N. Sanes, L. Pizzamiglio, Spatial coding of visual and somatic sensory information in body-centred coordinates, Eur. J. Neurosci. 14 (4) (2001) 737–746, https://doi.org/10.1046/J.0953-816X.2001.01674.X.

[22] C. Gaser, R. Dahnke, CAT-a computational anatomy toolbox for the analysis of structural MRI data, Hbm 2016 (2016) 336–348.

[23] R. Gattu, F.W. Akin, A.T. Cacace, C.D. Hall, O.D. Murnane, E.M. Haacke, Vestibular, balance, microvascular and white matter neuroimaging characteristics of blast injuries and mild traumatic brain injury: four case reports, Brain Inj. 30 (12) (2016) 1501–1514, https://doi.org/10.1080/02699052.2016.1219056.

[24] Z. Hadi, Y. Pondeca, E. Calzolari, M. Mahmud, M. Chepisheva, R.M. Smith, H. Rust, D.J. Sharp, B.M. Seemungal, The human brain networks mediating the vestibular sensation of self-motion, BioRxiv 2021 (2022), https://doi.org/10.1101/2021.12.03.471139, 12.03.471139.

[25] C. Helmchen, B. Machner, M. Rother, P. Spliethoff, M. Göttlich, A. Sprenger, Effects of galvanic vestibular stimulation on resting state brain activity in patients with bilateral vestibulopathy, Hum. Brain Mapp. 41 (9) (2020) 2527–2547, https://doi.org/10.1002/HBM.24963.

[26] M. Hitier, S. Besnard, P.F. Smith, Vestibular pathways involved in cognition, Front. Integr. Neurosci. 8 (JUL) (2014), https://doi.org/10.3389/FNINT.2014.00059.

[27] Y. Huang, S.K. Bailey, P. Wang, L.E. Cutting, J.C. Gore, Z. Ding, Voxel-wise detection of functional networks in white matter, NeuroImage 183 (2018) 544–552, https://doi.org/10.1016/j.neuroimage.2018.08.049.

[28] Y. Huang, Y. Yang, L. Hao, X. Hu, P. Wang, Z. Ding, J.H. Gao, J.C. Gore, Detection of functional networks within white matter using independent component analysis, NeuroImage 222 (2020), 117278, https://doi.org/10.1016/j.neuroimage.2020.117278.

[29] S. Imbaud Genieys, Vertigo, dizziness and falls in the elderly, Ann. Otolaryngol. Chir. Cervicofac. 124 (4) (2007) 189–196, https://doi.org/10.1016/j.aorl.2007.04.003.

[30] P. Kahane, D. Hoffmann, L. Minotti, A. Berthoz, Reappraisal of the human vestibular cortex by cortical electrical stimulation study, Ann. Neurol. 54 (5) (2003) 615–624, https://doi.org/10.1002/ana.10726.

[31] D. Kaski, S. Quadir, Y. Nigmatullina, P.A. Malhotra, A.M. Bronstein, B. M. Seemungal, Temporoparietal encoding of space and time during vestibular-

guided orientation, Brain 139 (2) (2016) 392–403, https://doi.org/10.1093/brain/awv370.
[32] V. Kirsch, D. Keeser, T. Hergenroeder, O. Erat, B. Ertl-Wagner, T. Brandt, M. Dieterich, Structural and functional connectivity mapping of the vestibular circuitry from human brainstem to cortex, Brain Struct. Funct. 221 (3) (2016) 1291–1308, https://doi.org/10.1007/s00429-014-0971-x.
[33] C.M. Lacadie, R.K. Fulbright, N. Rajeevan, R.T. Constable, X. Papademetris, More accurate Talairach coordinates for NeuroImaging using nonlinear registration, NeuroImage 42 (2) (2008) 717, https://doi.org/10.1016/J.NEUROIMAGE.2008.04.240.
[34] F. Latini, J. Mårtensson, E.M. Larsson, M. Fredrikson, F. Åhs, M. Hjortberg, H. Aldskogius, M. Ryttlefors, Segmentation of the inferior longitudinal fasciculus in the human brain: a white matter dissection and diffusion tensor tractography study, Brain Res. 1675 (2017) 102–115, https://doi.org/10.1016/j.brainres.2017.09.005.
[35] M. Li, Y. Gao, F. Gao, A.W. Anderson, Z. Ding, J.C. Gore, Functional engagement of white matter in resting-state brain networks, NeuroImage 220 (2020), 117096, https://doi.org/10.1016/j.neuroimage.2020.117096.
[36] S. Liu, J.D. Dickman, D.E. Angelaki, Response dynamics and tilt versus translation discrimination in Parietoinsular vestibular cortex, Cereb. Cortex 21 (3) (2011) 563–573, https://doi.org/10.1093/CERCOR/BHQ123.
[37] G. Macauda, M. Moisa, F.W. Mast, C.C. Ruff, L. Michels, B. Lenggenhager, Shared neural mechanisms between imagined and perceived egocentric motion – a combined GVS and fMRI study, Cortex 119 (2019) 20–32, https://doi.org/10.1016/J.CORTEX.2019.04.004.
[38] L. Marussich, K.H. Lu, H. Wen, Z. Liu, Mapping white-matter functional organization at rest and during naturalistic visual perception, NeuroImage 146 (2017) 1128–1141, https://doi.org/10.1016/j.neuroimage.2016.10.005.
[39] S. Mori, K. Oishi, H. Jiang, L. Jiang, X. Li, K. Akhter, K. Hua, A.V. Faria, A. Mahmood, R. Woods, A.W. Toga, G.B. Pike, P.R. Neto, A. Evans, J. Zhang, H. Huang, M.I. Miller, P. van Zijl, J. Mazziotta, Stereotaxic white matter atlas based on diffusion tensor imaging in an ICBM template, NeuroImage 40 (2) (2008) 570–582, https://doi.org/10.1016/j.neuroimage.2007.12.035.
[40] K. Murphy, R.M. Birn, D.A. Handwerker, T.B. Jones, P.A. Bandettini, The impact of global signal regression on resting state correlations: are anti-correlated networks introduced? NeuroImage 44 (3) (2009) 893–905, https://doi.org/10.1016/j.neuroimage.2008.09.036.
[41] T.E. Nichols, Multiple testing corrections, nonparametric methods, and random field theory, NeuroImage 62 (2) (2012) 811–815, https://doi.org/10.1016/J.NEUROIMAGE.2012.04.014.
[42] Y. Nigmatullina, P.J. Hellyer, P. Nachev, D.J. Sharp, B.M. Seemungal, The neuroanatomical correlates of training-related perceptuo-reflex uncoupling in dancers, Cereb. Cortex 25 (2) (2015) 554–562, https://doi.org/10.1093/cercor/bht266.
[43] S. Ogawa, D.W. Tank, R. Menon, J.M. Ellermann, S.G. Kim, H. Merkle, K. Ugurbil, Intrinsic signal changes accompanying sensory stimulation: functional brain mapping with magnetic resonance imaging, Proc. Natl. Acad. Sci. U. S. A. 89 (13) (1992) 5951–5955, https://doi.org/10.1073/pnas.89.13.5951.
[44] K. Oishi, K. Zilles, K. Amunts, A. Faria, H. Jiang, X. Li, K. Akhter, K. Hua, R. Woods, A.W. Toga, G.B. Pike, P. Rosa-Neto, A. Evans, J. Zhang, H. Huang, M.I. Miller, P.C. M. van Zijl, J. Mazziotta, S. Mori, Human brain white matter atlas: identification and assignment of common anatomical structures in superficial white matter, NeuroImage 43 (3) (2008) 447–457, https://doi.org/10.1016/j.neuroimage.2008.07.009.
[45] S.S. Panesar, F.C. Yeh, T. Jacquesson, W. Hula, J.C. Fernandez-Miranda, A quantitative tractography study into the connectivity segmentation laterality of the human inferior longitudinal fasciculus, Front. Neuroanat. 12 (2018), https://doi.org/10.3389/fnana.2018.00047.
[46] M. Patel, Y. Nigmatullina, B.M. Seemungal, J.F. Golding, A.M. Bronstein, Effects of prochlorperazine on normal vestibular ocular and perceptual responses: a randomised, double-blind, crossover, placebo-controlled study, Audiol. Neuro-Otol. 19 (2) (2014) 91–96, https://doi.org/10.1159/000357028.
[47] M. Peer, M. Nitzan, A.S. Bick, N. Levin, S. Arzy, Evidence for functional networks within the human brain's white matter, J. Neurosci. 37 (27) (2017) 6394–6407, https://doi.org/10.1523/JNEUROSCI.3872-16.2017.
[48] J.D. Power, K.A. Barnes, A.Z. Snyder, B.L. Schlaggar, S.E. Petersen, Spurious but systematic correlations in functional connectivity MRI networks arise from subject motion, NeuroImage 59 (3) (2012) 2142–2154, https://doi.org/10.1016/j.neuroimage.2011.10.018.
[49] R.E. Roberts, H. Ahmad, Q. Arshad, M. Patel, D. Dima, R. Leech, B.M. Seemungal, D.J. Sharp, A.M. Bronstein, Functional neuroimaging of visuo-vestibular interaction, Brain Struct. Funct. 222 (5) (2017) 2329–2343, https://doi.org/10.1007/s00429-016-1344-4.
[50] C. Rorden, M. Brett, Stereotaxic display of brain lesions, Behav. Neurol. 12 (4) (2000) 191–200, https://doi.org/10.1155/2000/421719.
[51] B.L. Rosario, A.L. Rosso, H.J. Aizenstein, T. Harris, A.B. Newman, S. Satterfield, S. A. Studenski, K. Yaffe, C. Rosano, Cerebral white matter and slow gait: contribution of hyperintensities and normal-appearing parenchyma, J. Gerontol. Series A Biol. Sci. Med. Sci. 71 (7) (2016) 968–973, https://doi.org/10.1093/gerona/glv224.
[52] B.M. Seemungal, The Mechanisms and Loci of Human Vestibular Perception, University of London, 2006. https://discovery.ucl.ac.uk/id/eprint/1445054/.
[53] B.M. Seemungal, I.A. Gunaratne, I.O. Fleming, M.A. Gresty, A.M. Bronstein, Perceptual and nystagmic thresholds of vestibular function in yaw, J. Vestib. Res. 14 (6) (2004) 461–466.
[54] B.M. Seemungal, V. Rizzo, M.A. Gresty, J.C. Rothwell, A.M. Bronstein, Posterior parietal rTMS disrupts human path integration during a vestibular navigation task, Neurosci. Lett. 437 (2) (2008) 88–92, https://doi.org/10.1016/j.neulet.2008.03.067.
[55] T. Sigurdsson, S. Duvarci, Hippocampal-prefrontal interactions in cognition, behavior and psychiatric disease, Front. Syst. Neurosci. 9 (JAN2016) (2016) 190, https://doi.org/10.3389/FNSYS.2015.00190/BIBTEX.
[56] A.T. Smith, M.B. Wall, K.V. Thilo, Vestibular inputs to human motion-sensitive visual cortex, Cereb. Cortex 22 (5) (2012) 1068–1077, https://doi.org/10.1093/CERCOR/BHR179.
[57] C. Sours, J. Zhuo, S. Roys, K. Shanmuganathan, R.P. Gullapalli, Disruptions in resting state functional connectivity and cerebral blood flow in mild traumatic brain injury patients, PLoS One 10 (8) (2015), https://doi.org/10.1371/JOURNAL.PONE.0134019.
[58] G. Spena, P. Gatignol, L. Capelle, H. Duffau, Superior longitudinal fasciculus subserves vestibular network in humans, NeuroReport 17 (13) (2006) 1403–1406, https://doi.org/10.1097/01.wnr.0000223385.49919.61.
[59] A. Stocco, C. Lebiere, R.C. O'Reilly, J.R. Anderson, Distinct contributions of the caudate nucleus, rostral prefrontal cortex, and parietal cortex to the execution of instructed tasks, Cogn. Affect. Behav. Neurosci. 12 (4) (2012) 611–628, https://doi.org/10.3758/s13415-012-0117-7.
[60] S. Whitfield-Gabrieli, A. Nieto-Castanon, Conn: a functional connectivity toolbox for correlated and Anticorrelated brain networks, Brain Connectivity 2 (3) (2012) 125–141, https://doi.org/10.1089/brain.2012.0073.
[61] A.M. Wirth, S.M. Frank, M.W. Greenlee, A.L. Beer, White matter connectivity of the visual-vestibular cortex examined by diffusion-weighted imaging, Brain Connectivity 8 (4) (2018) 235–244, https://doi.org/10.1089/brain.2017.0544.
[62] T. Womelsdorf, S. Everling, Long-range attention networks: circuit motifs underlying endogenously controlled stimulus selection, Trends Neurosci. 38 (11) (2015) 682–700, https://doi.org/10.1016/J.TINS.2015.08.009.
[63] E.J. Woytowicz, C. Sours, R.P. Gullapalli, J. Rosenberg, K.P. Westlake, Modulation of working memory load distinguishes individuals with and without balance impairments following mild traumatic brain injury, Brain Inj. 32 (2) (2018) 191–199, https://doi.org/10.1080/02699052.2017.1403045.
[64] S. Yakubovich, S. Israeli-Korn, O. Halperin, G. Yahalom, S. Hassin-Baer, A. Zaidel, Visual self-motion cues are impaired yet overweighted during visual–vestibular integration in Parkinson's disease, Brain Commun. 2 (1) (2020), https://doi.org/10.1093/BRAINCOMMS/FCAA035.
[65] N. Yousif, H. Bhatt, P.G. Bain, D. Nandi, B.M. Seemungal, The effect of pedunculopontine nucleus deep brain stimulation on postural sway and vestibular perception, Eur. J. Neurol. 23 (3) (2016) 668–670, https://doi.org/10.1111/ene.12947.
[66] H. Zhang, T.E. Nichols, T.D. Johnson, Cluster mass inference via random field theory, NeuroImage 44 (1) (2009) 51–61, https://doi.org/10.1016/J.NEUROIMAGE.2008.08.017.
[67] D.C. Zhu, T. Covassin, S. Nogle, S. Doyle, D. Russell, R.L. Pearson, J. Monroe, C. M. Liszewski, J.K. DeMarco, D.I. Kaufman, A potential biomarker in sports-related concussion: brain functional connectivity alteration of the default-mode network measured with longitudinal resting-state fMRI over thirty days, J. Neurotrauma 32 (5) (2015) 327–341, https://doi.org/10.1089/NEU.2014.3413.
[68] B.M. Seemungal, The cognitive neurology of the vestibular system, Curr Opin Neurol. 27 (1) (2014) 125–132, https://doi.org/10.1097/WCO.0000000000000060.
[69] B.M. Seemungal, et al., Vestibular activation differentially modulates human early visual cortex and V5/MT excitability and response entropy, Cereb. Cortex 23 (1) (2013) 12–19, https://doi.org/10.1093/cercor/bhr366.
[70] K. Jumani, J. Powell, Benign Paroxysmal Positional Vertigo: Management and Its Impact on Falls, Ann. Otol. Rhinol. Laryngol. 126 (8) (2017) 602–605, https://doi.org/10.1177/0003489417718847.
[71] A. Kleinschmidt, K.V. Thilo, C. Büchel, M.A. Gresty, A.M. Bronstein, R.S. J. Frackowiak, Neural Correlates of Visual-Motion Perception as Object- or Self-motion, NeuroImage 16 (4) (2002) 873–882, https://doi.org/10.1006/nimg.2002.1181.